

# Effects of cavity-field statistics on atomic entanglement

Biplab Ghosh,\* A. S. Majumdar,<sup>†</sup> and N. Nayak<sup>‡</sup>  
*S. N. Bose National Centre for Basic Sciences, Salt Lake, Kolkata 700 098, India*  
(Dated: December 2, 2024)

We study the entanglement properties of a pair of two-level atoms going through a cavity one after another. The initial joint state of two successive atoms that enter the cavity is unentangled. Interactions mediated by the cavity photon field result in the final two-atom state being of a mixed entangled type. We consider respectively various field statistics as in the Fock state field, thermal field, coherent state field and squeezed state field inside the cavity, and calculate the entanglement of formation, the well-known measure appropriate for mixed states, of the joint two-atom state as a function of the Rabi-angle  $gt$ . We present a detailed and comparative study of two-atom entanglement for low and high mean photon number cases corresponding to the different cavity fields.

PACS numbers: 03.67.-a, 03.65.Ud

## I. Introduction

The most interesting idea associated with composite quantum systems is quantum entanglement. A pair of particles is said to be entangled in quantum mechanics if its state cannot be expressed as a product of the states of its individual constituents. This was first noted by Einstein, Podolsky and Rosen in 1935[1]. The preparation and manipulation of these entangled states that have nonclassical and nonlocal properties leads to a better understanding of basic quantum phenomena. For example, complex entangled states, such as the Greenberger, Horne, and Zeilinger triplets of particles[2] are used for tests of quantum nonlocality[3]. Beyond these fundamental aspects, entanglement has become a fundamental resource in quantum information processing[4] and there has been rapid development of this subject in recent years[5].

Entanglement has been widely observed within the framework of quantum optical systems such as cavity quantum electrodynamics. Many beautiful experiments have been carried out, and in recent years, entangled states have been created and verified. Practical realization of various features of quantum entanglement are obtained in atom-photon interactions in optical and microwave cavities[6]. An example that could be highlighted is the generation of a maximally entangled state between two modes in a single cavity using a Rydberg atom coherently interacting with each mode in turn[7]. For practical implementation of quantum information protocols useful in communication and computation[5], entanglement has to be created and preserved between qubits that are well separated, and a recent experimental breakthrough has been obtained by entangling two distant atomic qubits by their interaction with the same

photon[8]. From the viewpoint of information processing, quantification of entanglement is an important aspect, and recently some studies have been performed to quantify the entanglement that is obtained in atom-photon interactions in cavities[9, 10, 11, 12].

In the present paper we will study the dynamical generation of entanglement between two two-level atoms mediated by various cavity fields. Since the atoms do not interact directly with each other, the properties of the radiation field encountered by them bears crucially on the nature of atomic entanglement. Our main purpose is to focus on the effect of different field dynamics on the magnitude of two-atom entanglement. We take the initial state of the two atoms as separate or product state and compute the entanglement generated between the atoms by the action of the cavity field encountered by the atoms while passing through the cavity one after the other. The interaction between the atom and the field is governed by the Jaynes-Cummings model[13] which is experimentally realizable. Note that there is no spatial overlap between the two atoms in this scheme, i.e., the two atoms never interact directly with each other. The generation of nonlocal correlations between the two atoms emerging from the cavity can in general be understood using the Horodecki theorem[14], and the joint two-atom state is known to violate Bell-type inequalities[15]. Since the joint state of the two atoms emanating from the cavity is not a pure state, we quantify the entanglement using the well-known measure appropriate for mixed states, i.e., the entanglement of formation[16]. We investigate how the statistics of different types of radiation fields influence the quantitative dynamics of atomic entanglement.

The structure of the paper is as follows. In Section II we review the interaction between two-level atom and single mode radiation field inside a cavity described by the Jaynes-Cummings model. We briefly discuss a quantifying technique for bipartite entanglement of a mixed quantum state, i.e., the entanglement of formation. In Section III we show how the entanglement between two spatially separated atoms is generated. We observe robust atom-atom entanglement mediated by the (a) Fock

\*Email:biplab@bose.res.in

<sup>†</sup>Email:archan@bose.res.in

<sup>‡</sup>Email:nayak@bose.res.in

state field, (b) thermal field, (c) coherent state field, and (d) squeezed field, respectively. We demonstrate how the various field statistics are reflected in two-atom entanglement for low and high average photon number states of the cavity fields. Several distinctive characteristics of the entanglement generated by the different fields are discussed. A common feature that is observed is that for the cavity low photon number case, the entanglement between the two atoms decreases with increasing average photon number of the field. We are also able to demonstrate that atomic entanglement can be quantitatively enhanced by the squeezing of the radiation field. A summary of our results and some concluding remarks are presented in Section IV.

## II. Entanglement mediated by the Jaynes-Cummings interaction

The Jaynes-Cummings (JC) model is one of the simplest examples of two interacting quantum systems. It is one of the most studied models in quantum optics because it is an exactly solvable model. Entanglement of the optical field with matter in the JC model has been studied earlier[17]. Here our aim is to study the entanglement between atoms mediated by the optical field, where the light-atom interaction is governed by the JC model. The JC model consists of a two-level atom coupled to a single-mode radiation field inside a cavity. A two level atom is formally analogous to a spin-1/2 system. Let us denote the upper level of the atom as  $|e\rangle$  and the lower level as  $|g\rangle$  and the spin (atomic) raising and lowering operators can be defined as  $\sigma^+ = |e\rangle\langle g|$  and  $\sigma^- = |g\rangle\langle e|$ , respectively, with the commutation relation

$$\begin{aligned} [\sigma^+, \sigma^-] &= |e\rangle\langle e| - |g\rangle\langle g| \\ &= \sigma_z. \end{aligned} \quad (1)$$

A quantum mechanical field can be represented as (for the present purpose, we consider a single mode field)

$$E(t) = \frac{1}{2}[ae^{-i\omega t} + a^\dagger e^{i\omega t}] \quad (2)$$

apart from a mode function which we omit here since it is not required for the present discussion. Here  $a$  and  $a^\dagger$  are annihilation and creation operators, respectively. The graininess of the radiation field is represented by the photon number state  $|n\rangle$ ,  $n = 0, 1, 2, \dots$ , such that  $a|n\rangle = \sqrt{n}|n-1\rangle$  and  $a^\dagger|n\rangle = \sqrt{n+1}|n+1\rangle$ . It is an eigenstate of the number operator  $\hat{n} = a^\dagger a$  given by

$$\hat{n}|n\rangle = n|n\rangle \quad (3)$$

The field in Eq.(2) can be represented by a quantum mechanical state vector  $|\psi\rangle$  which is a linear superposition of the number states  $|n\rangle$ , i.e.,

$$|\psi\rangle = \sum_{n=0}^{\infty} c_n |n\rangle \quad (4)$$

where  $c_n$  is, in general, complex and gives the probability of the field having  $n$  photons by the relation

$$P_n = \langle n|\psi\rangle\langle\psi|n\rangle = |c_n|^2 \quad (5)$$

The field obeys quantum statistics and its average photon number is given by

$$\langle n \rangle = \sum_{n=0}^{\infty} n P_n \quad (6)$$

with the intensity of the field  $I \propto \langle n \rangle$ . The statistics brings in a quantum mechanical noise which is represented by the variance

$$V = \frac{\langle n^2 \rangle - \langle n \rangle^2}{\langle n^2 \rangle}. \quad (7)$$

$V = 1$  is for coherent state field and  $V < 1$  signifies a non-classical state. The parameters  $\langle n \rangle$  and  $V$  give a fair description of the quantum mechanical nature of the radiation field. However, a squeezed field [18] needs same extra parameters which we will present when we will arrive at the discussion of its effect on entanglement.

The Hamiltonian of the joint atom-field system can be written in the rotating wave approximation [19] as,

$$H = \frac{\omega\sigma_z}{2} + a^\dagger a\omega + g(\sigma^+ a + \sigma^- a^\dagger), \quad (8)$$

where  $a^\dagger$  and  $a$  are usual creation and destruction operators of the radiation field. (Here we have set  $\hbar = 1$ ). In the interaction picture, the equation of motion defining the system is

$$i\frac{\partial}{\partial t}|\psi_{a-f}(t)\rangle_I = H_{int}^I|\psi_{a-f}(t)\rangle_I, \quad (9)$$

where the Hamiltonian reduces to

$$H_I = g(\sigma^+ a + \sigma^- a^\dagger). \quad (10)$$

Here we have considered the quality factor of the cavity  $Q = \infty$  since the cavity-QED related experiments are carried out with cavities with very high  $Q$  [6]. However, the field statistics influences the dynamics governed by the Eq.(9). We shall consider the cavity field to be in a Fock, thermal, coherent or squeezed state, respectively.

With the passage of the two atoms, one after the other, the joint state of both the atoms and the field at some instance  $t$  may be denoted by  $|\Psi(t)\rangle_{a-a-f}$ . The corresponding atom-atom-field pure density state is

$$\rho(t) = |\Psi(t)\rangle\langle\Psi(t)| \quad (11)$$

In order to quantify the entanglement between the two atoms, the field variables have to be traced out. The reduced mixed density state of two atoms after taking trace over the field is

$$\rho(t) = \text{Tr}_{\text{field}}(|\Psi(t)\rangle\langle\Psi(t)|) \quad (12)$$

Entanglement within pure states of bipartite system can be measured by the Von Neumann entropy of the reduced density matrices. Various measures have been introduced to quantify bipartite entanglement of mixed states but none of them satisfies all the requisite criteria for an axiomatically sound measure [20]. While the entanglement for a mixed state can be measured as the average entanglement of its pure state decompositions, the existence of an infinite number of such decompositions makes their minimization over this set a nontrivial task. Hill and Wootters [16] carried out such a procedure for bipartite,  $2 \otimes 2$  systems and showed that a quantity ‘entanglement of formation’ is a measure of entanglement. The entanglement of formation has since turned out to be a popular measure for computing atomic entanglement in quantum optical systems[8, 9, 10, 11, 12]. The entanglement of formation for a bipartite density operator  $\rho$  is given by

$$E_F(\rho) = h \left( \frac{1 + \sqrt{1 - C^2(\rho)}}{2} \right), \quad (13)$$

where  $C$  is called the concurrence defined as

$$C(\rho) = \max(0, \sqrt{\lambda_1} - \sqrt{\lambda_2} - \sqrt{\lambda_3} - \sqrt{\lambda_4}), \quad (14)$$

where the  $\lambda_i$  are the eigenvalues of  $\rho_{12}(\sigma_y \otimes \sigma_y)\rho_{12}^*(\sigma_y \otimes \sigma_y)$  in descending order, and

$$h(x) = -x \log_2 x - (1-x) \log_2(1-x) \quad (15)$$

is the binary entropy function. The entanglement of formation is a monotone of the concurrence. Clearly,  $E_F = 0$  for  $C = 0$ .

### III. Entanglement features of cavity fields

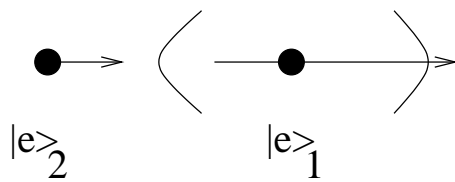


FIG. 1: Two atoms prepared in excited states are pass through a single mode cavity one after the other.

We consider a micromaser system in which atoms are sent into the cavity at such a rate that the probability of two atoms being present there is negligibly small. Our purpose here is to show the influence of the photon statistics of the driving fields (radiation field with which the atoms interact) on atomic entanglement. For this sake, we consider the cavity to be of a non-leaky type, that is,  $Q = \infty$ . In fact, the cavity-QED experiments are very close to such situations[6]. In the following, we consider

various kinds of radiation fields. First, we consider a Fock state field to show the effect of a photon number state  $|n\rangle$  ( $n \propto I$ , the intensity of the field) on atomic entanglement. Next, we consider linear superpositions of  $|n\rangle$  which can be a thermal field [21], or a coherent state field [22]. Finally we study the effect of the squeezing properties[18] of the radiation field on the entanglement.

#### A. FOCK STATE FIELD

A Fock state is written as  $|n\rangle$  with  $n$  an integer value, signifying that there are  $n$  quanta of excitation in the mode.  $|0\rangle$  corresponds to the ground state (no excitation). Fock states form the most convenient basis of the Fock space. The amplitudes  $c_n$  in Eq.(4) obey the delta function relation

$$c_n = \delta_{m,n} \quad (16)$$

where  $m$  is the photon number of the Fock state. The variance is given by

$$V = 1 - \frac{1}{m}. \quad (17)$$

So, for small values of  $m$ ,  $V < 1$  and field has non-classical character. For large  $m$ ,  $V$  tends towards the classical limit. This feature is reflected in the entanglement generated between the two atoms, as we shall see later.

Let us first consider the passage of the first atom, initially in the excited state  $|e\rangle$ , through the cavity. The joint atom-field state is given by

$$|\Psi(t=0)\rangle_{a-f} = |e\rangle \otimes |n\rangle. \quad (18)$$

The atom-field wave function evolves with the interaction given by Eqs.(9) and (10) to

$$|\Psi(t)_{a-f}\rangle = \cos(\sqrt{n+1}gt)|e, n\rangle + \sin(\sqrt{n+1}gt)|g, n+1\rangle \quad (19)$$

The next atom which enters the cavity interacts with this “changed” field and thus a correlation develops between the two atoms via the cavity field. The joint state of the two atoms and the field is given by

$$|\Psi(t)\rangle_{a-a-f} = \alpha_1|e_1, e_2, n\rangle + \alpha_2|e_1, g_2, n+1\rangle + \alpha_3|g_1, e_2, n+1\rangle + \alpha_4|g_1, g_2, n+2\rangle \quad (20)$$

where

$$\begin{aligned} \alpha_1 &= \cos^2(\sqrt{n+1}gt), \\ \alpha_2 &= \cos(\sqrt{n+1}gt)\sin(\sqrt{n+1}gt), \\ \alpha_3 &= \cos(\sqrt{n+2}gt)\sin(\sqrt{n+1}gt), \\ \alpha_4 &= \sin(\sqrt{n+1}gt)\sin(\sqrt{n+2}gt). \end{aligned} \quad (21)$$

The corresponding atom-atom-field pure density state is

$$\rho(t)_{a-a-f} = |\Psi(t)\rangle_{a-a-f} \langle \Psi(t)| \quad (22)$$

The reduced mixed density state of two atoms after tracing over the field is given by (we display the non-vanishing terms only)

$$\begin{aligned} \rho(t)_{a-a} &= \text{tr}_f(\rho(t)_{a-a-f}) \\ &= \alpha_1^2 |e_1 e_2\rangle \langle e_1 e_2| + \alpha_2^2 |e_1 g_2\rangle \langle e_1 g_2| \\ &\quad + \alpha_3^2 |g_1 e_2\rangle \langle g_1 e_2| + \alpha_2 \alpha_3 |e_1 g_2\rangle \langle g_1 e_2| \\ &\quad + \alpha_2 \alpha_3 |g_1 e_2\rangle \langle e_1 g_2| + \alpha_4^2 |g_1 g_2\rangle \langle g_1 g_2|. \end{aligned} \quad (23)$$

We compute the entanglement of formation  $E_F$  given by Eq.(13) for this bipartite two-atom state. In Figure 2  $E_F$  is plotted versus the Rabi angle  $gt$  for different values of  $n$ .

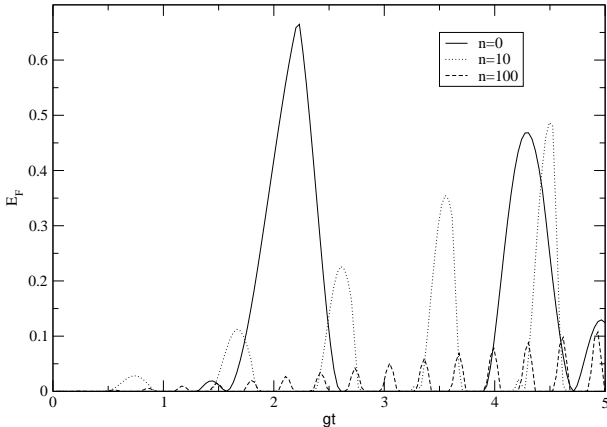


FIG. 2: Atom-atom entanglement versus  $gt$ . Solid line, dotted line, and dashed line indicate  $E_F$  between two atoms when the cavity fock states are  $n = 0$ ,  $n = 10$ , and  $n = 100$  respectively.

The peaks of the entanglement of formation are reflective of the photon statistics that are typical in micromaser dynamics[23]. We see that  $E_F$  falls off sharply as  $n$  increases. The non-classical character of the field for small values of the average photon number  $n$  as indicated by Eq.(7), is reflected in larger entanglement between the two atoms. An interesting comparison can be made with the case of the Tavis-Cummings model[24] which is employed when two atoms are present simultaneously inside the cavity. Although simultaneous interaction of two excited atoms with Fock state field never results in two-atom entanglement as was shown by Tessier et al. [12], the notable difference here is that in the JC dynamics modelling the micromaser one always gets two-atom entanglement mediated by the Fock state cavity field, as we see in Figure 2.

## B. THERMAL FIELD

The thermal field is the most easily available radiation field, and so, its influence on the entanglement of spins is of much interest. The field at thermal equilibrium obeying Bose-Einstein statistics has an average photon number at temperature  $T^0 K$ , given by

$$\langle n \rangle = \frac{1}{e^{\hbar\omega/kT} - 1}. \quad (24)$$

The photon statistics is governed by the distribution  $P_n$  given by

$$P_n = \frac{\langle n \rangle^n}{(1 + \langle n \rangle)^{n+1}}. \quad (25)$$

This distribution function always peaks at zero, i.e.,  $n_{peak} = 0$ .

We are considering a system in which the two atoms are sent into the cavity one after the other. For a thermal field distribution function for the cavity field, the joint two-atom-cavity state is obtained by summing over all  $n$ , and is given by

$$\begin{aligned} |\Psi(t)\rangle_{a-a-f} &= \sum_n A_n [\cos^2(\sqrt{n+1}gt)|e_1, e_2, n\rangle \\ &\quad + \cos(\sqrt{n+1}gt)\sin(\sqrt{n+1}gt)|e_1, g_2, n+1\rangle \\ &\quad + \cos(\sqrt{n+2}gt)\sin(\sqrt{n+1}gt)|g_1, e_2, n+1\rangle \\ &\quad + \sin(\sqrt{n+1}gt)\sin(\sqrt{n+2}gt)|g_1, g_2, n+2\rangle] \end{aligned} \quad (26)$$

where  $P_n = |A_n|^2$  is the photon distribution function of the thermal field given by Eq.(25).

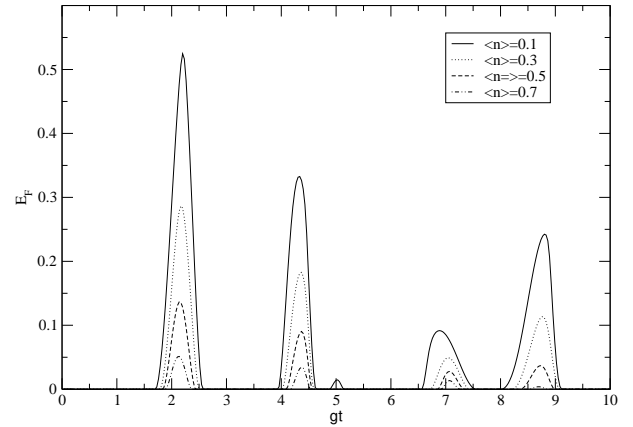


FIG. 3: Atom-atom entanglement of formation mediated by the thermal cavity field is plotted versus  $gt$ .

The reduced mixed density state of two atoms after passing through the thermal cavity field can be written as

$$\rho(t)_{a-a} = \text{tr}_f(\rho(t)_{a-a-f})$$

$$\begin{aligned} \beta_1 |e_1 e_2\rangle \langle e_1 e_2| + \beta_2 |e_1 g_2\rangle \langle e_1 g_2| \\ + \beta_3 |g_1 e_2\rangle \langle g_1 e_2| + \beta_4 |e_1 g_2\rangle \langle g_1 e_2| \\ + \beta_5 |g_1 g_2\rangle \langle g_1 g_2|, \end{aligned} \quad (27)$$

where

$$\begin{aligned} \beta_1 &= \sum_n P_n \cos^4(\sqrt{n+1}gt), \\ \beta_2 &= \sum_n P_n \cos^2(\sqrt{n+1}gt) \times \\ &\quad \sin^2(\sqrt{n+1}gt), \\ \beta_3 &= \sum_n P_n \cos^2(\sqrt{n+2}gt) \times \\ &\quad \sin^2(\sqrt{n+1}gt), \\ \beta_4 &= \sum_n P_n \sin^2(\sqrt{n+1}gt) \times \\ &\quad \cos(\sqrt{n+1}gt) \cos(\sqrt{n+2}gt), \\ \beta_5 &= \sum_n P_n \sin^2(\sqrt{n+1}gt) \times \\ &\quad \sin^2(\sqrt{n+2}gt). \end{aligned} \quad (28)$$

We compute the entanglement of formation  $E_F$  for the above two-atom state and plot it versus the Rabi angle  $gt$  for different values of average photon number  $\langle n \rangle$  in Figure 3.. It is interesting to note that the thermal field which has minimal information can nevertheless entangle qubits that are prepared initially in a separable state. In the context of the Tavis-Cummings framework when both the atoms interact simultaneously with the radiation field, Kim et al. [11] have noticed similar trends in the entanglement mediated by the thermal field. Thus both Jaynes-Cummings and the Tavis-Cummings models of atom-photon interaction generate similar entanglement when the radiation field is thermal, whereas for the coherent field case the situation is contrasting as observed earlier.

### C. COHERENT STATE FIELD

A more appropriate basis for many optical fields are coherent states. A coherent states contains an indefinite number of photons and is a minimum uncertainty state[20] standing at the threshold of the classical-quantum limit. These states are parametrised by a single complex number  $\alpha$  as follows:

$$|\alpha\rangle = \sum_n \frac{\alpha^n}{\sqrt{n!}} |n\rangle. \quad (29)$$

A coherent state is an eigenstate of the annihilation operator  $a$  written as

$$a|\alpha\rangle = \alpha|\alpha\rangle \quad (30)$$

and obeys a Poissonian distribution function in the photon number representation given by

$$P_n = \frac{e^{-\langle n \rangle} \langle n \rangle^n}{n!} \quad (31)$$

with the average photon number  $\langle n \rangle = |\alpha|^2$ . The distribution function  $P_n$  peaks at non-zero photon number, i.e.,  $n_{peak} \neq 0$ .

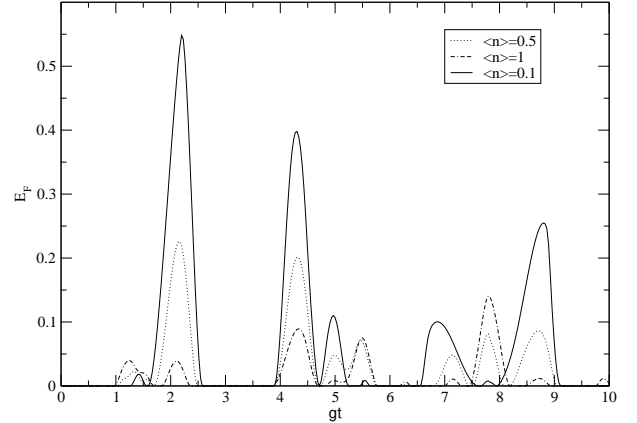


FIG. 4: Two-atom entanglement mediated by the coherent state cavity field at low average photon number is plotted versus  $gt$ .

For a coherent state field distribution function for the cavity field, the total state of the two atoms and the cavity field is given by

$$\begin{aligned} |\Psi(t)\rangle_{a-a-f} = \sum_n A_n [\cos^2(\sqrt{n+1}gt)|e_1, e_2, n\rangle \\ + \cos(\sqrt{n+1}gt) \sin(\sqrt{n+1}gt)|e_1, g_2, n+1\rangle \\ + \cos(\sqrt{n+2}gt) \sin(\sqrt{n+1}gt)|g_1, e_2, n+1\rangle \\ + \sin(\sqrt{n+1}gt) \sin(\sqrt{n+2}gt)|g_1, g_2, n+2\rangle] \end{aligned} \quad (32)$$

where  $P_n = |A_n|^2$  is the photon distribution function of the coherent state field.

The reduced mixed density state of the two atoms after passing through the cavity field can be written in the matrix form in the basis of  $|e_1\rangle, |e_2\rangle, |g_1\rangle$  and  $|g_2\rangle$  states as

$$\rho_{a-a} = \begin{pmatrix} \gamma_1 & \gamma_7 & \gamma_8 & \gamma_6 \\ \gamma_7 & \gamma_2 & \gamma_4 & \gamma_9 \\ \gamma_8 & \gamma_4 & \gamma_3 & \gamma_{10} \\ \gamma_6 & \gamma_9 & \gamma_{10} & \gamma_5 \end{pmatrix}. \quad (33)$$

where

$$\begin{aligned} \gamma_1 &= \sum_n P_n \cos^4(\sqrt{n+1}gt), \\ \gamma_2 &= \sum_n P_n \cos^2(\sqrt{n+1}gt) \times \end{aligned}$$

$$\begin{aligned}
& \sin^2(\sqrt{n+1}gt), \\
\gamma_3 &= \sum_n P_n \cos^2(\sqrt{n+2}gt) \times \\
& \sin^2(\sqrt{n+1}gt), \\
\gamma_4 &= \sum_n P_n \sin^2(\sqrt{n+1}gt) \times \\
& \cos(\sqrt{n+1}gt) \cos(\sqrt{n+2}gt), \\
\gamma_5 &= \sum_n P_n \sin^2(\sqrt{n+1}gt) \times \\
& \sin^2(\sqrt{n+2}gt), \\
\gamma_6 &= \sum_n \sqrt{P_n P_{n-2}} \cos^2(\sqrt{n+1}gt) \times \\
& \sin(\sqrt{n}gt) \sin(\sqrt{n-1}gt), \\
\gamma_7 &= \sum_n \sqrt{P_n P_{n-1}} \cos^2(\sqrt{n+1}gt) \times \\
& \cos(\sqrt{n}gt) \sin(\sqrt{n}gt), \\
\gamma_8 &= \sum_n \sqrt{P_n P_{n-1}} \cos^3(\sqrt{n+1}gt) \times \\
& \sin(\sqrt{n}gt), \\
\gamma_9 &= \sum_n \sqrt{P_n P_{n-1}} \sin^2(\sqrt{n+1}gt) \times \\
& \cos(\sqrt{n+1}gt) \sin(\sqrt{n}gt), \\
\gamma_{10} &= \sum_n \sqrt{P_n P_{n-1}} \sin^2(\sqrt{n+1}gt) \times \\
& \cos(\sqrt{n+2}gt) \sin(\sqrt{n}gt). \tag{34}
\end{aligned}$$

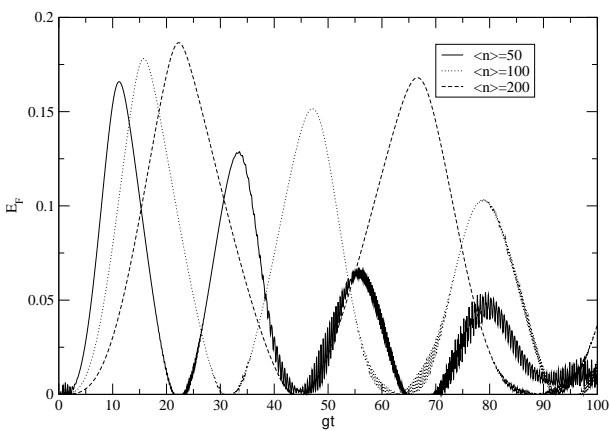


FIG. 5: Atom-atom entanglement mediated by coherent state cavity field at high average photon number is plotted versus  $gt$ .

We compute the entanglement of formation  $E_F$  for low and high photon numbers separately as the two cases have distinctive features for the coherent state field.  $E_F$  is plotted versus the Rabi angle  $gt$  for low average photon

number  $< n >$  in Figure 4. For small photon numbers,  $n_{peak} \approx 0$  and hence, the evolution of  $E_F$  is similar to that in the thermal field case. For large  $< n >$ ,  $n_{peak}$  moves significantly to the right (Figure 5) and its influence is completely different compared to that for the low  $< n >$  case. Quantum effects which are predominant primarily when the photon number is low, help to increase the peak value of  $E_F$ . We note in Figure 5 that in general,  $E_F$  increases slightly with  $< n >$  with its time evolution being different for different  $< n >$ . This is reminiscent of the collapse-revival characteristic in the Jaynes-Cummings model[21, 23]. We further note that though  $E_F$  is higher for the low photon number category (Figure 4), this behaviour is reversed for the high photon number category (Figure 5). For high  $< n >$ , the features of generated entanglement are thus significantly different from those in the case of the thermal field.

#### D. SQUEEZED RADIATION FIELD

A class of minimum-uncertainty states are known as squeezed states. In general, a squeezed states have less noise in one quadrature than a coherent state. To satisfy the requirements of a minimum-uncertainty state the noise in the other quadrature is greater than that of a coherent state. Coherent states are a particular category of a more general class of minimum uncertainty states with equal noise in both quadratures. Recently, there have been some proposals of the connection of the squeezing parameter with the entanglement of atomic states[25]. Our purpose here is to study what effect squeezing of the radiation field has on the entanglement of a pair of atoms passing through it.

The electric field in the Eq.(2) can be written as

$$E(t) = a_1 \cos \omega t + a_2 \sin \omega t \tag{35}$$

where  $a_1 = (a + a^\dagger)/2$  and  $a_2 = (a - a^\dagger)/2i$  are the two quadratures satisfying  $[a_1, a_2] = i/2$ . The variances  $\Delta a_1 = \sqrt{< a_1^2 > - < a_1 >^2}$  and  $\Delta a_2 = \sqrt{< a_2^2 > - < a_2 >^2}$  satisfy

$$\Delta a_1 \Delta a_2 \geq \frac{1}{4}. \tag{36}$$

The coherent state or the minimum uncertainty state given by Eqs.(29-31) satisfy the equality sign along with

$$\Delta a_1 = \Delta a_2 = \frac{1}{2}. \tag{37}$$

Further, either of  $\Delta a_1$  or  $\Delta a_2$  can be reduced below  $\frac{1}{2}$  at the expense of the other such that Eq. (36) is satisfied, and radiation fields having such properties are called squeezed fields.

The photon distribution function of the squeezed radiation field can be represented as

$$P_n = \frac{1}{n! \mu} \left( \frac{\nu}{2\mu} \right)^n e^{-\beta^2(\frac{\nu}{\mu}-1)} |H_n(\frac{\beta}{\sqrt{2\mu\nu}})|^2, \tag{38}$$

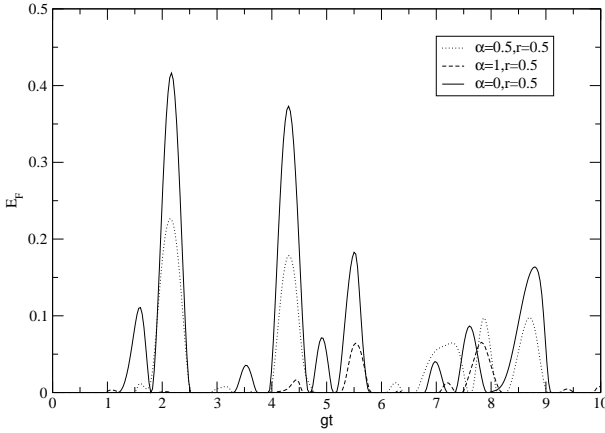


FIG. 6: Atom-atom entanglement of formation mediated by the squeezed field for different values of  $\alpha$  is plotted versus  $gt$  for the low photon number case.

where  $\beta$  is related to the coherent state amplitude  $\alpha$  in Eq.(30) by  $\beta = (\mu + \nu)\alpha$  for real  $\alpha$ .  $\mu$  and  $\nu$  can be represented by the squeezing parameter  $r$  as  $\mu = \cosh r$  and  $\nu = \sinh r$ . The average photon number can thus be written as

$$\langle n \rangle = |\alpha|^2 + \sinh^2 r. \quad (39)$$

In terms of the squeezing parameter, the variances of such fields are given by

$$\begin{aligned} \Delta a_1 &= \frac{1}{2} e^{-r}, \\ \Delta a_2 &= \frac{1}{2} e^r. \end{aligned} \quad (40)$$

Clearly, for  $r = 0$ , the statistics reduce to that for a coherent state given by Eq.(31).  $r > 0$  gives rise to sub-Poissonian statistics, whereas  $r < 0$  produces a super-Poissonian field.

As, in the previous cases, we first obtain the reduced density matrix corresponding to the joint two-atom state after passing through a cavity with the squeezed field. The reduced density matrix has a similar form to that of the coherent state field given by Eq.(33), where  $\gamma^s$  are also of the same form as given in Eq.(34). The difference in this case arises from the different photon statistics  $P_n$  obtained from the squeezed field distribution function as given in Eq.(38).

The effects of the photon statistics of the squeezed field on two-atom entanglement for low average photon number are displayed in the Figures 6 and 7, for varying  $\alpha$  and  $r$ , respectively. We see that for low photon numbers, the time evolution of  $E_F$  is similar to that for a

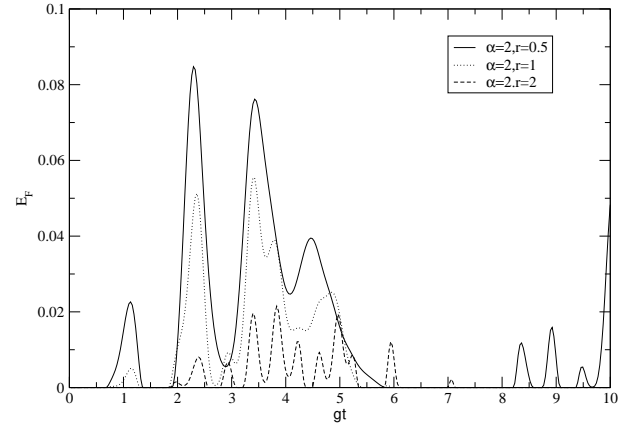


FIG. 7:  $E_F$  mediated by the squeezed field is plotted versus  $gt$  for different values of the squeezing parameter  $r$  corresponding to the low average photon number case.

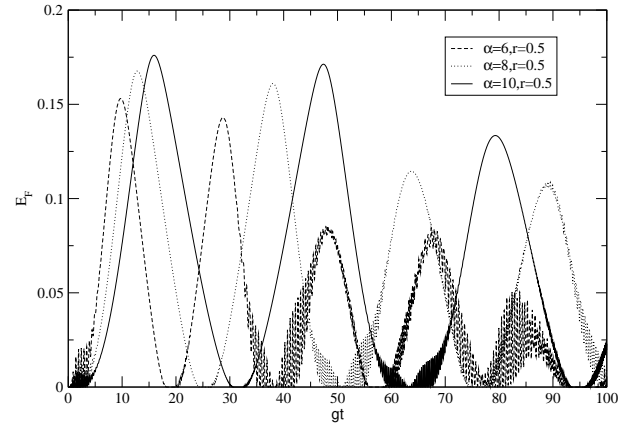


FIG. 8:  $E_F$  mediated by squeezed field for different values of  $\alpha$  is plotted versus  $gt$  for the high average photon number case.

thermal or coherent field. The effect of the squeezing parameter  $r$  enters through  $\langle n \rangle$  in Eq.(39). An increase in  $r$  increases  $\langle n \rangle$  and thus  $E_F$  diminishes accordingly. It might appear from Figure 7 that squeezing of the radiation field is anti-correlated with the generated atomic entanglement, but what is actually reflected here is the decrease of  $E_F$  caused by the increase of the average photon number  $\langle n \rangle$ . We emphasize on this point since later (Figure 9) we will indeed see that by squeezing the field but holding  $\langle n \rangle$  fixed, one can increase the atomic entanglement of formation. The situation for the high photon number case resembles that for the coherent state field. This is seen in Figure 8 where a larger value of  $\alpha$  corresponds to a larger  $\langle n \rangle$ , and causes  $E_F$  to be slightly increased with increasing  $n$  or  $\alpha$ .

#### IV. Summary and Discussions

Before concluding, it is instructive to perform a comparative computation of  $E_F$  mediated by the various cavity radiation fields for the same average photon number  $\langle n \rangle$ . In Figures 9 and 10 we plot the two-atom entanglement of formation  $E_F$  versus the Rabi angle  $gt$  separately for the thermal state, coherent state, and the squeezed state, respectively, but keeping the average cavity photon number fixed. In Figure 9 we see that for small  $\langle n \rangle$ , the dynamics of  $E_F$  are similar for all kinds of cavity fields. By lowering the average photon number  $\langle n \rangle$ , the two-atom entanglement  $E_F$  reduces. The quantitative difference in reduction stems from the different statistics for the various fields. As expected, the least magnitude of entanglement is mediated by the thermal field. The striking feature of Figure 9 is in the peaks of  $E_F$  for various values of  $gt$ . Note that  $E_F$  for the squeezed field (dotted line) is higher compared to the coherent state field (dashed line). Thus squeezing of the radiation field as represented by the non-vanishing value of the squeezing parameter  $r$ , leads to a notable increase in the magnitude of atomic entanglement over the case the coherent state field ( $r = 0$ ; no squeezing). This trend is also visible in the high photon number case (Figure 10), though not for all values of  $gt$ . Another notable feature exhibited in Figure 10 is that the thermal field is unable to mediate atomic entanglement at high values of the cavity photon number  $\langle n \rangle$ .

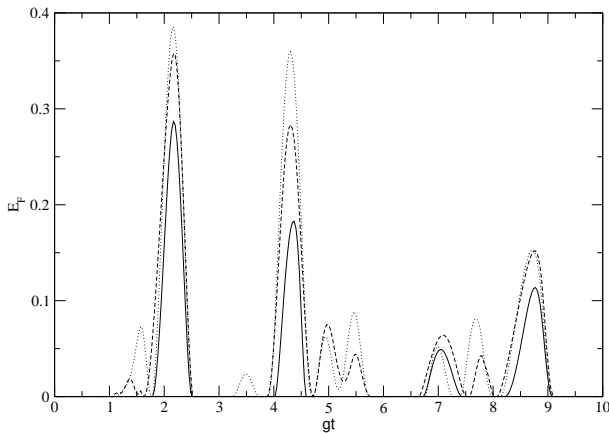


FIG. 9: Atom-atom entanglement mediated by (i) squeezed cavity field (dotted line) when  $\langle n \rangle = 0.3$  and  $r = 0.5$ , (ii) coherent state field (dashed line) when  $\langle n \rangle = 0.3$ , and (iii) thermal field (solid line) when  $\langle n \rangle = 0.3$ , plotted vs  $gt$ .

To summarize, in this paper we have presented a realistic micromaser-type model where two spatially separated atoms are entangled via a cavity field. The entanglement between the two separate atoms builds up via atom-photon interactions inside the cavity, even though no single atom interacts directly with another. We have

computed the two-atom entanglement as measured by the entanglement of formation  $E_F$ , for the case of four different types of radiation fields, i.e., the Fock state field, the thermal field, the coherent state field, and the squeezed field. Our purpose has been to study the effects of the statistics of the bosonic radiation field on the dynamics of the entanglement of two atomic qubits, i.e., two fermionic systems. Several interesting features of atomic entanglement are observed.

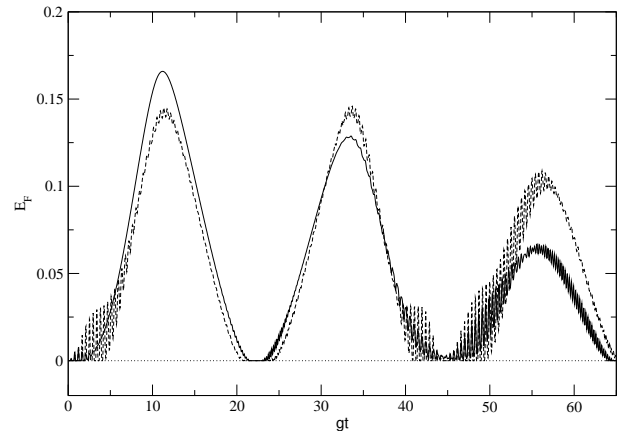


FIG. 10: Atom-atom entanglement mediated by (i) squeezed cavity field (dashed line) when  $\langle n \rangle = 50$  and  $r = 1$ , (ii) coherent state field (solid line) when  $\langle n \rangle = 50$ , and (iii) thermal field (dotted line) when  $\langle n \rangle = 50$ , plotted vs  $gt$ .

We first show that for the Fock state cavity field, entanglement between two successively passing atoms can be generated as a consequence of Jaynes-Cummings (JC) dynamics. This is in contrast to the case when both the atoms reside together inside the cavity when Tavis-Cummings (TC) dynamics for atom-photon interactions is unable to generate atomic entanglement[12]. We then study the entanglement mediated by the thermal radiation field. It is interesting to note that the thermal field which carries minimum information is still able to produce atomic entanglement through both the JC interaction as seen here, and also through the TC interaction as was observed earlier[11]. However, the thermal field having a high value of the average photon number loses its ability to entangle atomic qubits passing through it. We next consider the coherent state field inside the cavity. Here two distinct patterns of entanglement are seen to emerge for the cases corresponding to low and high average cavity photon numbers respectively. In the former case the quantum nature of the radiation field plays a prominent role in enhancing atomic entanglement with the decrease of  $\langle n \rangle$ . The situation reverses for high  $\langle n \rangle$  case where actually the increase of  $\langle n \rangle$  leads to a slight increase of  $E_F$ . We finally investigate the effect of squeezing of the radiation field on entanglement. Here again the behaviour of entanglement can be cate-

gorized in two different regimes, i.e., the low and high  $\langle n \rangle$  cases separately, similar to the situation for the coherent state field. The key feature observed is that the two-atom entanglement can be increased with squeezing if the average photon number is held fixed.

Finally, we would like to reemphasize that the quantitative study of entanglement produced in various types of atom-photon interactions is a relevant arena for investigations. Atom-photon interactions and the generation of entanglement mediated through them are expected to play an important role in possible future practical realizations in the field of quantum communications[8, 26].

The properties of different radiation fields in controlled environments such as that of cavity-QED can be used to manipulate the interactions with atomic qubits[27] and hence control the entanglement produced. Recently, the possibility of entanglement of a thermal radiation field with high temperature phonons associated with moving mirrors of a cavity has been shown[28], brightening the prospects for creating macroscopic entanglement. Even from a purely pedagogical perspective, investigations of quantitative entanglement in atom-photon interactions could lead to interesting insights on the curious properties of entanglement such as its ‘monogamous’ nature[29].

---

[1] A. Einstein, B. Podolsky and N. Rosen, Phys. Rev. **47**, 777 (1935).

[2] D. M. Greenberger, M. A. Horne, and A. Zeilinger, Am. J. Phys. **58**, 1131 (1990).

[3] J. W. Pan, D. Bouwmeester, M. Daniell, H. Weinfurter and A. Zeilinger, Nature (London) **403**, 515 (2000).

[4] C. H. Bennett, G. Brassard, C. Crpeau, R. Jozsa, A. Peres, and W. K. Wootters Phys. Rev. Lett. **70**, 1895 (1993); M. Zukowski, A. Zeilinger, M. A. Horne and A. K. Ekert, Phys. Rev. Lett. **71**, 4287 (1993).

[5] See, for example, M. A. Nielsen and I. L. Chuang, *Quantum Computation and Information* (Cambridge University Press, Cambridge, England, 2000).

[6] J. M. Raimond, M. Brune and S. Haroche, Rev. Mod. Phys. **73**, 565 (2001).

[7] A. Rauschenbeutel, P. Bertet, S. Osnaghi, G. Nogues, M. Brune, J. M. Raimond and S. Haroche, Phys. Rev. A **64**, 050301 (2001).

[8] D. N. Matsukevich, T. Chanelire, S. D. Jenkins, S.-Y. Lan, T. A. B. Kennedy, and A. Kuzmich, Phys. Rev. Lett. **96**, 030405 (2006).

[9] P. Masiak, Phys. Rev. A **66**, 023804 (2002).

[10] A. Datta, B. Ghosh, A. S. Majumdar and N. Nayak, Europhys. Lett. **67**, 934 (2004).

[11] M. S. Kim, Jinhyoung Lee, D. Ahn and P. L. Knight, Phys. Rev. A **65**, 040101(R) (2002); L. Zhou, H. S. Song and C. Li, J. Opt. B: Quantum Semiclass. Opt. **4**, 425 (2002).

[12] T. Tessier, A. Delgado, I. Fuentes-Guridi, and I. H. Deutsch, Phys. Rev. A **68**, 062316 (2003).

[13] E. T. Jaynes, F. W. Cummings, Proc. IEEE **51**, 89 (1963).

[14] Horodecki et al., Phys. Lett. A, **200**, 340 (1995).

[15] A. S. Majumdar and N. Nayak, Phys. Rev. A **64**, 013821 (2001).

[16] S. Hill and W. K. Wootters, Phys. Rev. Lett. **78**, 5022 (1997); W. K. Wootters, Phys. Rev. Lett. **80** 2245 (1998).

[17] S. J. D. Phoenix and P. L. Knight, Annals of Physics **186**, 381 (1988); E. Boukobza and D. J. Tannor, quant-ph/0505119.

[18] D. F. Walls, Nature **324**, 210 (1986).

[19] See, for instance, W. H. Louisell, *Quantum Statistical Properties of Radiation* (Wiley, New York, 1973).

[20] M. Keyl, Phys. Rep. **369**, 431 (2002).

[21] N. Nayak, Opt. Commun. **118** 114 (1995).

[22] R. J. Glauber, Phys. Rev. B **1**, 2766 (1963).

[23] N. Nayak, A. S. Majumdar and V. Bartzis, Nonlinear Optics **24**, 319 (2000).

[24] M. Tavis and F. W. Cummings, Phys. Rev. **170**, 379 (1968).

[25] A. Sorensen, L. M. Duan, J. I. Cirac and P. Zoller, Nature **409**, 63 (2001); A. Banerjee, quant-ph/0110032; J. K. Korbicz, J. I. Cirac and M. Lewenstein, Phys. Rev. Lett. **95**, 120502 (2005).

[26] J. Volz, M. Weber, D. Schlenk, W. Rosenfeld, J. Vrana, K. Saucke, C. Kurtsiefer, and H. Weinfurter, Phys. Rev. Lett. **96**, 030404 (2006).

[27] A. Biswas and G. S. Agarwal, Phys. Rev. A **69**, 062306 (2004).

[28] A. Ferreira, A. Guerreiro, and V. Vedral, Phys. Rev. Lett. **96**, 060407 (2006).

[29] B. Ghosh, A. S. Majumdar, and N. Nayak, quant-ph/0505037 (to appear in Int. J. Quant. Inf.).